CHAPTER 189

FIELD VERIFICATION OF A NUMERICAL MODEL OF BEACH TOPOGRAPHY CHANGE DUE TO NEARSHORE CURRENTS, UNDERTOW AND WAVES

Takuzo Shimizu [1], Masahito Tsuru [1] and Akira Watanabe [2]

ABSTRACT

A practical method for estimating the undertow velocity and its direction is developed and verified on the basis of field measurement data. It is found that a simple vector addition of nearshore current and undertow gives a good approximation.

The actual bottom topography change during a year is simulated by the 3-D beach evolution model taking into account the cross-shore sediment transport due to waves and undertow as well as the transport due to nearshore currents. The results of both measurements and calculations show that the sediment transport due to nearshore current is predominant and the contribution of cross-shore sediment transports is cancelled for a long-term beach evolution.

INTRODUCTION

The sediment transport due to nearshore currents plays a predominant roll on the long-term beach evolution and the contribution of cross-shore sediment transports due to waves and undertow is usually cancelled for a long period beyond approximately a year. In many cases for prediction of long-term beach topography changes due to construction of a coastal structure, only the sediment transport due to nearshore currents is taken into account. The shoreline model based on this concept is also widely used in practice. Therefore, the 3-D beach evolution model which treats only the sediment transport due to nearshore currents, can be regarded as an improved version of the shoreline model, which has

[1]Penta-Ocean Construction Co. Ltd. , 2-2-8 Koraku, Bunkyo-ku, Tokyo 112, Japan.
[2]Professor, Dept. of Civil Eng., Univ. of Tokyo, 7-3-1 Hongo, Bunkyo-ku, Tokyo 113, Japan.

an advantage of predicting the spatial beach topography changes.

In recent years, we have applied the 3-D beach evolution model based on this concept to many practical problems and presented a few attempts to quantitatively demonstrate its field applicability through comparisons with the actual topographical changes around harbors (e.g. Shimizu et al., 1990). It is well known, on the other hand, that the offshoreward sediment transport due to undertow in the surf zone and the onshoreward sediment transport due to sheet flow movement outside the surf zone causes a considerable beach profile change and form a bar during the storm. Most of the previous studies on the undertow and its effects on beach profile changes have been conducted mainly through laboratory experiments and are not thoroughly discussed on the basis of field measurement data.

In this study, at first, we discuss the undertow velocity and its direction through comparisons between the field mesurement data and the calculated nearshore currents and, then, discuss their practical estimation method. We also try to simulate the actual bottom topography changes during approximately a year by taking into account the cross-shore sediment transport due to waves and undertow as well as the sediment transport due to nearshore currents.

FIELD INVESTIGATION

Fig. 1 shows the bottom topography of the investigation site and the calculation area which is 0.9km long in the alongshore direction and 1.0km long in the cross-shore direction with the grid spacing of 12.5m. The field investigation site is located at the end of a sandy pocket beach. The bottom slope is approximately 1/40. A part of the shore is bounded directly by the sea cliff, and the bottom slope is steep near the shoreline. The bottom contours are straight and parallel to the shoreline outside the harbor, and they extend offshoreward like a tongue around the harbor entrance owing to extreme accretion caused by nearshore currents. The seabed material is well-sorted fine sands in the nearshore region where the water depth is less than 10m, and the grain diameter is approximately 0.35mm.

The field observation was carried out over a period of approximately one month during the winter stormy season, in order to obtain the data for verification of the numerical models for estimation of nearshore waves and currents. At Points 1 to 4 with the water depth of about 5m, the mean currents including nearshore currents and undertow and principal wave direction were measured at the level of 0.7m above the bottom by using electro-magnetic current meters. At Points 2 and 4, nearshore waves were also measured by pressure sensors attached to the electro-magnetic current meters. The incident wave conditions were also measured at Point 0 with the water depth of 20m by using a combination of an ultrasonic wave gauge and an electro-magnetic current meter. Data were recorded with the sampling interval of 0.5 seconds during 10 minutes every 2 hours. The pressure fluctuations obtained by a pressure sensor were converted into water

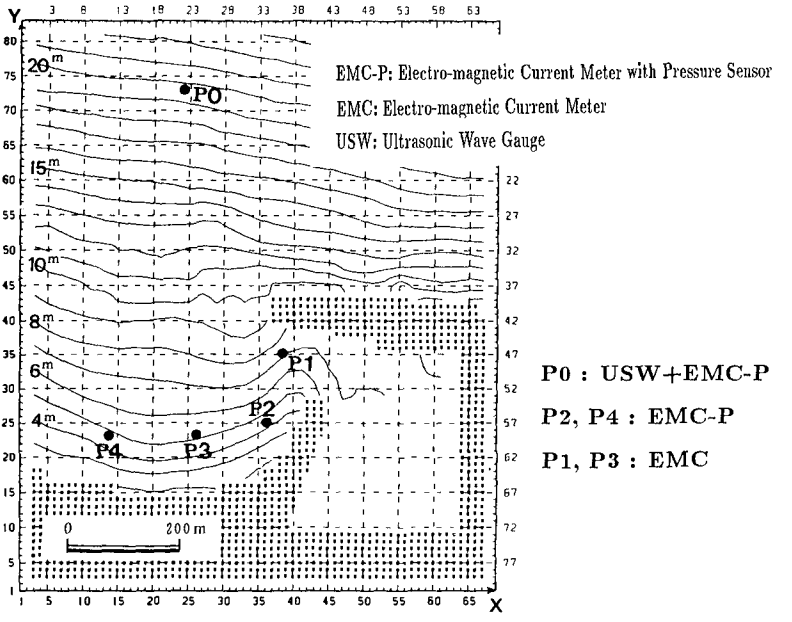

Fig. 1 Bottom topography and calculation area of investigation site.

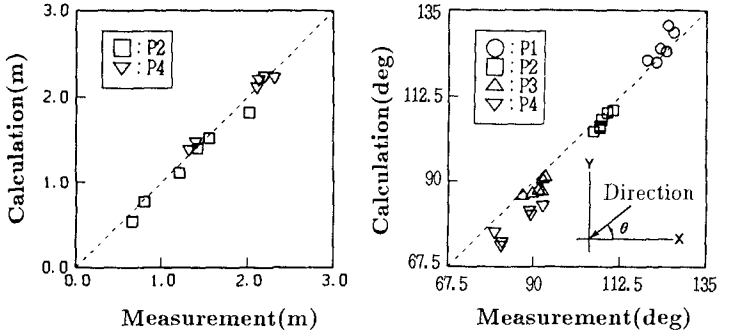

(a) $H_{1/3}$ (b) θ_p

Fig. 2 Comparisons between the measured and the calculated significant wave heights and principal directions.

surface motion on the basis of the small amplitude wave theory. During the observation, storm waves greater than 3m in significant wave height attacked twice. The maximum significant wave height was 4.2m and its period was 9.6s.

VERIFICATION OF WAVE MODEL

The Employed Wave Model

The parabolic-type equation model proposed by Isobe(1987) is employed in this study to properly estimate the wave field around the harbor entrance where combined diffraction and refraction occur. This basic equation is derived from the mild slope equation and the energy dissipation term due to wave breaking is included. The parabolic-type equation model has advantages that much computational time can be saved owing to the forward stepping scheme, and then, treatment of multi-directional irregular waves is easy. Random waves are described as a superposition of component regular waves with different frequencies and directions.

In order to improve the accuracy of calculating the wave transformation for a wide range of propagation directions of component waves, a curvilinear coordinate system is introduced. In this model, the curvilinear coordinates are defined from the peak frequency and the peak direction of the directional wave spectrum. In a shadow region, additional wave rays are radiated from the tip of the breakwater. The applicabilities of the model to the actual wave field over complicated bottom topographies were verified through comparisons with field measurement data (Shimizu et al., 1992, 1994).

Comparison of Wave Height and Direction

In order to compare the calculations with the measurements, the incident wave conditions measured at Point 0 are classified into three cases in accordance with the wave height level ($H_{1/3}$ (P0): $\sim$ 2.0m, 2.0 $\sim$ 3.0m, 3.0m $\sim$) and two cases of wave direction, the righthand side and the lefthand side directions to that perpendicular to the shoreline. For totally six cases of incident wave conditions, the mean values of significant wave height and principal direction were calculated at all measurement points. And these values were adopted as the field verification data. The numerical calculations were also conducted for the mean significant waves of these six cases, using the Bretschneider-Mitsuyasu frequency spectrum and the Mitsuyasu-type directional distribution function.

Fig. 2 (a) and (b) show the comparisons between the measured and the calculated significant wave heights and principal directions. The calculations of both significant wave height and principal direction by the parabolic-type equation model show fairly good agreements with the measurements.

VERIFICATION OF UNDERTOW AND NEARSHORE CURRENT MODEL

Field Observation Results

Fig. 3 (a) shows an example of the comparisons between the measured steady component vectors of near-bottom velocity and the calculated nearshore current vectors under the same wave condition with the significant wave height of 3.5m. The bold vectors are measurements and illustrated in a different scale from the calculated vectors. In calculating the nearshore current field of random waves, the radiation stress is evaluated as for a regular wave with the equivalent wave energy and the principal direction.

During the storm, the wave-induced nearshore circulation develops around the harbor entrance behind the main breakwater. Extreme accretion around the harbor entrance is caused mainly by this nearshore circulation. Around the harbor entrance, the calculated nearshore current field satisfactorily reproduces the observed dominant nearshore circulation.

On the contrary, at Point 4 where there is no influence of diffraction due to breakwater, when the significant wave height becomes larger than 2m and

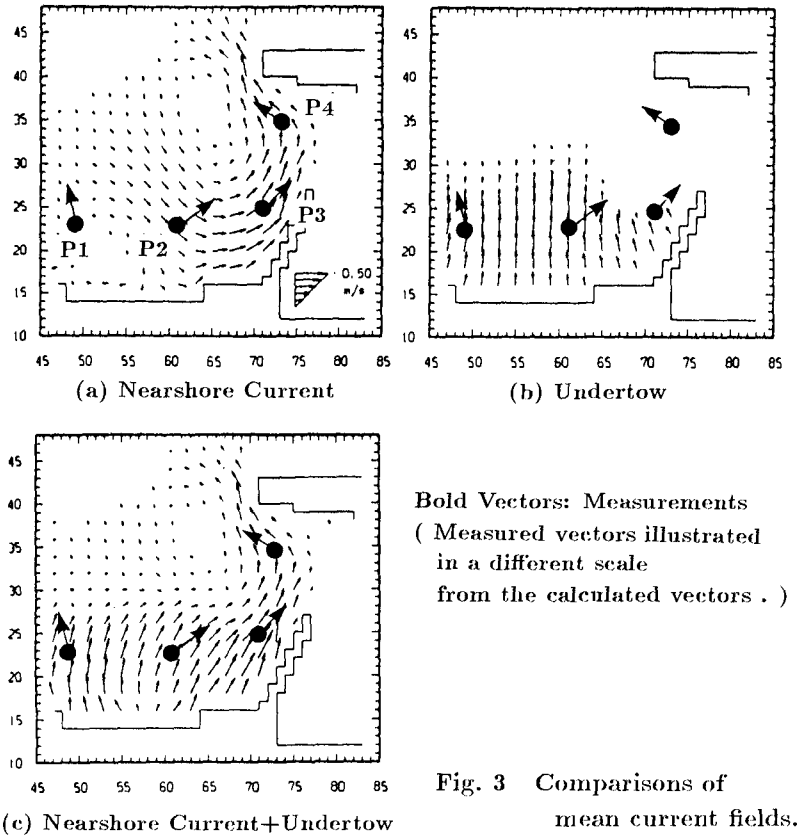

(a) Nearshore Current (b) Undertow

(c) Nearshore Current+Undertow

Bold Vectors: Measurements
(Measured vectors illustrated in a different scale from the calculated vectors .)

Fig. 3 Comparisons of mean current fields.

the measurement point is involved in the surf zone, the remarkable offshoreward mean currents occur and the velocity becomes larger than 0.3m/s. Even at Point 3 where the nearshore circulation occur, the mean current vector slaightly inclines offshoreward. The sensors of the electro-magnetic current meters were installed at the level of 0.7m above the bottom and at the water depth of about 5m and, then, they were always located under the trough level. The observed offshoreward mean current, therefore, seems to be due to undertow.

Estimation Method of Undertow

The undertow velocity is estimated as the sum of the return flows compensating for the onshore mass flux due to breaking bores and due to irrotational wave motion and the Eulerian mass transport velocity. We adopt the following rough estimation of the undertow velocity due to breaking bores after Sato et al.(1988).

$$U_b = -A\frac{H^2}{d \cdot T} \tag{1}$$

where A is a nondimensional coefficient, H the wave height, d the water depth and T the wave period. For random waves, assuming that only breaking waves contribute to generation of return flow, H^2 is replaced by the breaking wave energy $E_b/(\rho g/8)$.

$$\frac{E_b}{\rho g/8} = \int_{x_b}^{\infty} H^2 p(\xi) d\xi = H_{rms}^2 \cdot P_b \tag{2}$$

$$P_b = (1 + x_b^2)\exp(-x_b^2) \tag{3}$$

where $x_b = H_b/H_{rms}$ and P_b is the probability of wave breaking which is estimated by assuming the Rayleigh distribution for individual waves. The root mean square wave height H_{rms} is estimated by not taking into account the wave breaking. The breaking wave Height H_b is evaluated by using the appropriate coefficient value, 0.14 in the wave breaker indices for regular waves proposed by Goda(1970). If the breaking wave energy estimated by this equation becomes larger than that estimated by the parabolic equation model with the additional term of energy dissipation due to wave breaking, the breaking wave energy is set to be the value estimated by the parabolic equation model.

In this study, it is assumed that the near-bottom mean current vector can be estimated by a simple vector addition of the nearshore current vector and the undertow vector after Svendsen and Lorenz(1989). The undertow vectors are given in the opposite direction of the local wave propagation.

Comparison of Undertow Due to Breaking Bores

Fig. 4 shows the relationship between the measured undertow velocity due to breaking bores U_b and the estimated values of $(H^2/d \cdot T)$, in order to calibrate the nondimensional coefficient A. The nearshore current vectors are given by the numerical calculations. The measured undertow velocity due to breaking bores $\vec{U_b}$ is evaluated by extracting the calculated nearshore current vector $\vec{U_c}$, the calculated return flow vector due to irrotational wave motion $\vec{U_w}$ and the calculated

Eulerian mass transport velocity $\vec{U_e}$ from the measured steady component vector of near-bottom velocity variation $\vec{U_m}$.

$$\vec{U_b} = \vec{U_m} - \vec{U_c} - (\vec{U_w} + \vec{U_e}) \tag{4}$$

The appropriate value of nondimensional coefficient A is found to be 5.6 through comparisons of the calculations with the measurements. This result is the same as the value obtained by Sato et al.(1988).

Fig. 5 shows the examples of the calculated cross-shore distributions of the significant wave height $H_{1/3}$, the breaking wave energy E_b and the undertow velocity U under the incident wave conditions with the significant wave height of 2.6m and 3.5m. The calculation results show that the undertow velocity increases exponetially and has a peak in the surf zone. The calculated wave heights and undertow velocities agree well with the measurements at Point 4.

Comparison of Mean Current

Fig. 3 (a) to (c) show the calculated mean current fields of nearshore current, undertow and the vector addition of both currents. Not only the nearshore circulation around the harbor entrance, but also the measured mean currents due to combined undertow and nearshore current are reproduced well by the simple vector addition. At Points 1 and 2 in the shadow region of the breakwater, the undertow velocity is small. At Points 3 and 4, on the other hand, where the incident waves directly attack, the undertow must be taken into account in order to properly estimate the mean current field during a storm.

Fig. 6 (a) and (b) show the comparisons between the measured and the calculated mean current velocities and between the measured and the calculated mean current directions at all measurement points. The open symbols indicate the calculations of only nearshore current, and the solid symbols indicate the calculations of a vector addition of nearshore current and undertow.

The calculations are the results conducted for the mean values of the incident significant waves observed at Point 0 for six cases in accordance with the incident wave height levels and the principal wave directions. The measurements are the mean values for six cases at each point. By a simple vector addition of nearshore current and undertow, both the calculated mean current velocity and its direction show fairly good agreements with the measured ones. The method for estimating the near-bottom mean current in the surf zone employed in this study is a simple and primitive, but it has enough accuracy for practical use.

VERIFICATION OF BEACH EVOLUTION MODEL

In order to verify the field applicability of the 3-D beach evolution model. We tried to reproduce the long-term topography changes around the harbor entrance during a year. Before completion of the construction of breakwaters, the bottom contours are parallel, and after the completion, they stretched like a tongue along

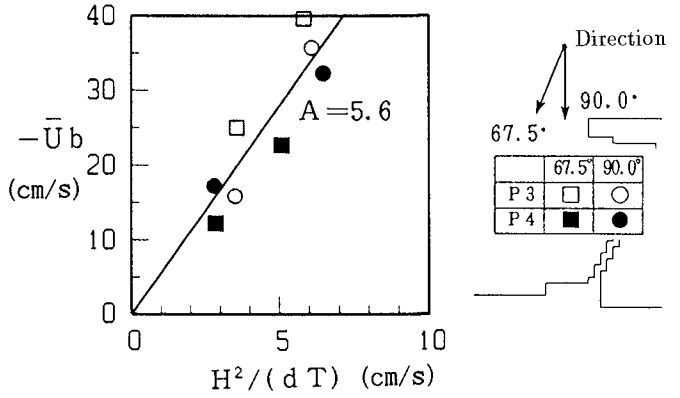

Fig. 4 Relationships between the undertow velocity due to breaking bores U_b and $(H^2/d \cdot T)$.

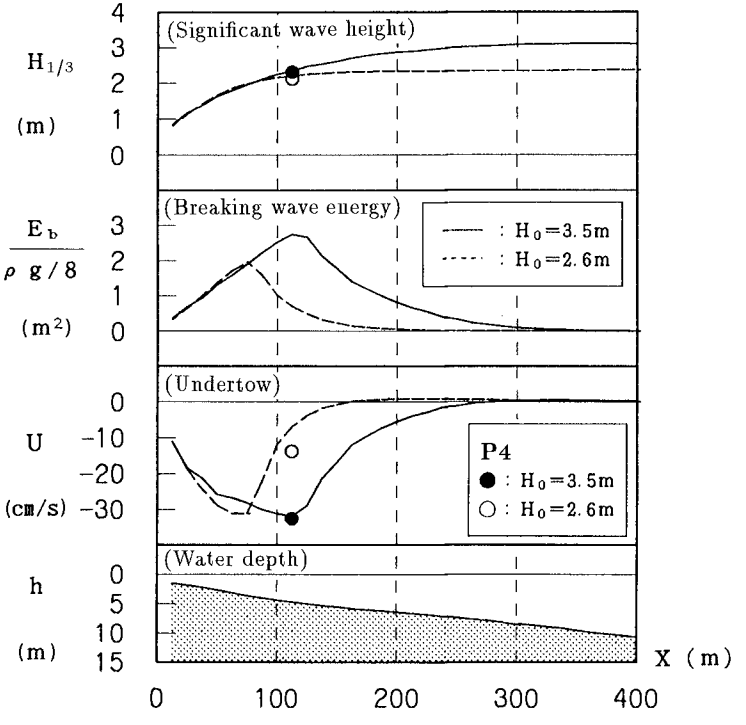

Fig. 5 Distributions of $H_{1/3}$, E_b and U(Undertow).

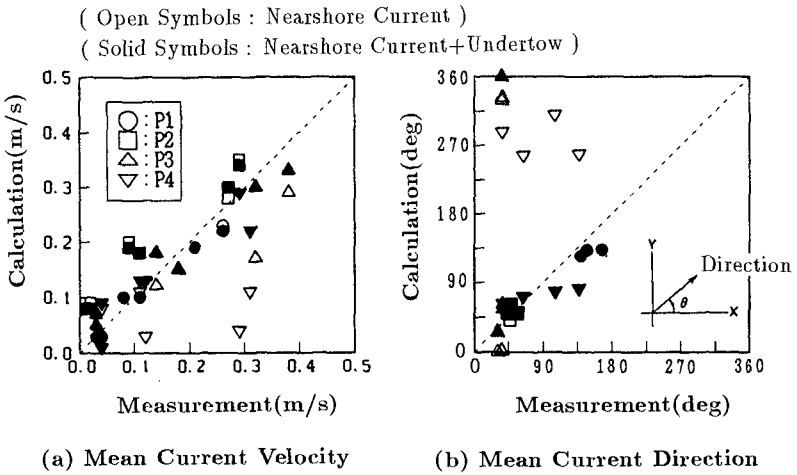

Fig. 6 Comparisons between the measured and the calculated mean current velocities and directions.

the sub-breakwater to the harbor entrance mainly owing to the nearshore circulation.

Sediment Transport Formula

The local sediment transport rate formula employed in this study is the formula proposed by Watanabe et al.(1986). The formula for local sediment transport rate under combined wave-current action is formulated so as to be consistent with previous studies on both longshore drift and cross-shore sediment transport. The transport rate $\vec{q}$ is divided into $\vec{q_c}$ due to mean currents and $\vec{q_w}$ due to waves. These formulas are based on the power model concept and assume that the sediments set in motion by the excess shear stress under combined wave-current action are transported with both mean currents and wave motion into the respective directions.

$$\vec{q_c} = A_c(\tau - \tau_c)\vec{U}/\rho g \tag{5}$$

$$\vec{q_w} = A_w F_D(\tau - \tau_c)\vec{u_b}/\rho g \tag{6}$$

where A_c and A_w are nondimensional coefficients, $\vec{U}$ the current velocity vector, $\vec{u_b}$ the maximum near-bottom orbital velocity vector, F_D a direction function for wave-induced net transport, τ the maximum bottom shear stress in a wave-current coexistent system, τ_c the critical shear stress for the onset of the general movement, ρ the water density, and g the gravity acceleration.

After Watanabe et al.(1991), the direction function for wave-induced net cross-shore sediment transport is set to be +1 for the onshoreward movements under

the Shields parameter less than 0.2 of the upper limit of bed load and larger than 0.5 of the onset of sheet flow movement, and is set to be -1 for the offshoreward movements of suspended load over ripples under the Shields parameter between 0.2 and 0.5. The bottom shear stress for a wave-current coexistent system is evaluated by the friction law proposed by Tanaka and Shuto(1981). The critical shear stress is calculated from the critical value of the Shields parameter, which is 0.11 for fine sands and 0.06 for coarse sands according to Watanabe et al.(1980).

The coefficient A_w in the formula for the transport due to wave action is related to another coefficient B_w in the formula for the wave-induced net sediment transport rate q_w proposed by Watanabe(1982), which is expressed as follows:

$$\phi = B_w(\psi - \psi_c)\psi^{1/2} \tag{7}$$

where $\phi = (1-\lambda_v)q_w/w_0 D$ is a dimensionless net transport rate, D, w_0 and λ_v are the diameter, settling velocity and porosity of the sediment, $\psi = \tau/(\rho_s - \rho)gD$ is the dimensionless shear stress or the Shields parameter, ρ_s and ρ are the densities of sediment and water, and ψ_c is the critical value of ψ for the onset of general movement of sediment.

The coefficient A_w is related to B_w as follows:

$$A_w/B_w = w_0\sqrt{f_w/2} \;/\; \{(1-\lambda_v)s\sqrt{sgD}\} \tag{8}$$

where f_w is the wave friction factor.

In the previous studies under the field conditions conducted by Watanabe et al.(1991), the value of B_w is considered to be approximately 3.0 to 5.0, though the coefficient must be calibrated in the field application. In this study, the value of B_w is set to be 2.0 after several tries and errors, and the value of A_w changes depending on local wave conditions and properties of sea-bed material. The value of A_c is set by multiplying the value of A_w by 10.0 after Watanabe et al.(1991).

Reproduction of Beach Topography Change

The numerical simulation was performed under a simply modelled series of wave conditions by repeating the calculations of waves, mean currents and beach topogaraphy changes. The wave conditions during the calibration period of approximately a year were replaced by the simply modelled four series of storms with the significant wave height larger than 2m as shown in Fig. 7. This modelled series of waves have the same occurrence frequency in total as that of the observed wave climate data.

Fig. 8 (a) shows the measured topographical changes and Fig. 8 (b) shows the calculated bottom topography changes by taking into account only the sediment transport due to nearshore currents. Remarkable accretion around the harbor entrance and erosion around Point 3 and at the tip of the breakwater due to nearshore circulation are reproduced satisfactorily. The results of both measurements and calculations show that the sediment transport due to nearshore current is predominant for the long-term beach evolution and that the contributions of

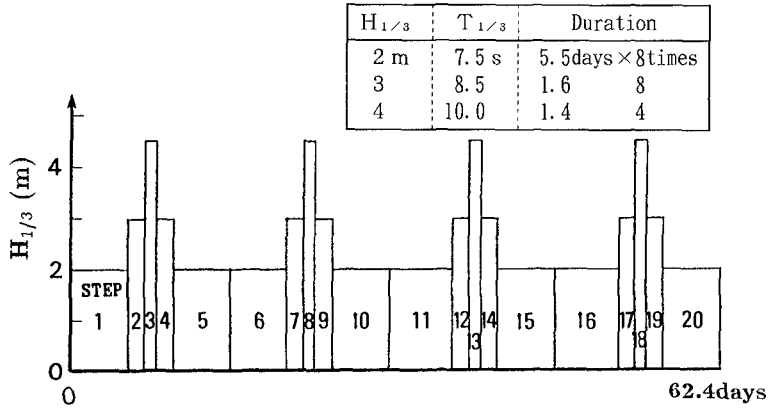

Fig. 7 Simply modelled series of incident wave conditions.

both the offshoreward sediment transport due to undertow and the onshoreward transport due to sheet flow are cancelled for a long-term beach profile change.

The difference between calculation and measurement is that the calculated result does not show such a sharp extension of the tongue-shaped bottom contours, for example the 4m contour, compared with the measurements. This fact suggests that the nearshore circulation is sharper and the width of fast current is narrower in the field than they are expected. In numerical calculation, however, it is difficult to reproduce such a sharp circulation as observed in the field, owing to the numerical diffusion.

Fig. 8 (c) shows the calculated bottom topography changes by taking into account the cross-shore sediment transport due to waves and undertow in addition to the transport due to nearshore currents. Around the harbor entrance, accretion due to nearshore current is reproduced well. In the area where waves attack directly and the cross-shore sediment transport is active during the storm, however, the measured topography changes are not reproduced well. In numerical calculation, the topographical changes due to cross-shore sediment transport is not cancelled even after a year.

We, therefore, tried to investigate more precisely the calculation results. Fig. 9 shows the examples of calculated bottom topography changes after 3rd to 5th step during the decreasing period of the wave height. The upper figures show changes during each step, and the lowers ones show the cumulative changes from the initial topography. The eroded area during 3rd step with the largest wave height is accreted during 4th step. And the eroded area during 4th step is accreted during 5th step. The eroded area near the shore due to severe waves is, thus, gradually buried and the accreted area moves onshoreward during the decreasing period of the storm. These results suggests that the wave-induced transport due to sheet flow and the flow-induced sediment transport due to undertow play an

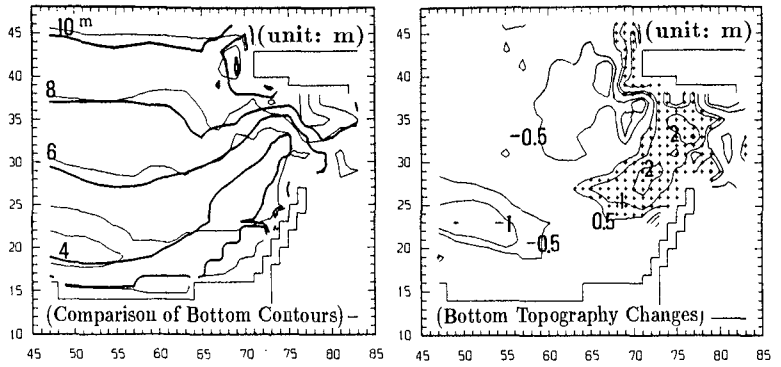

(a) Measurement

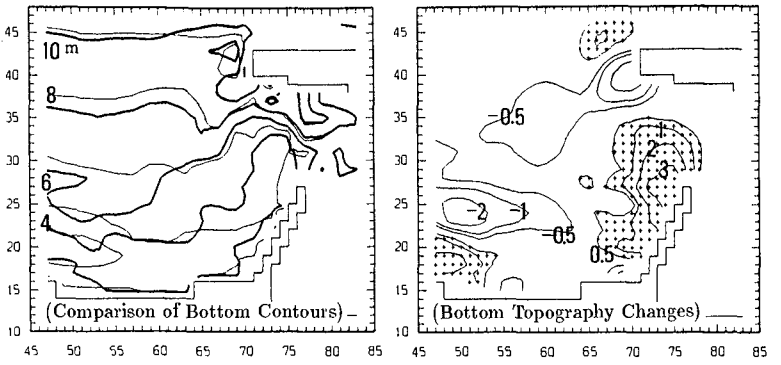

(b) Calculation (Nearshore Current)

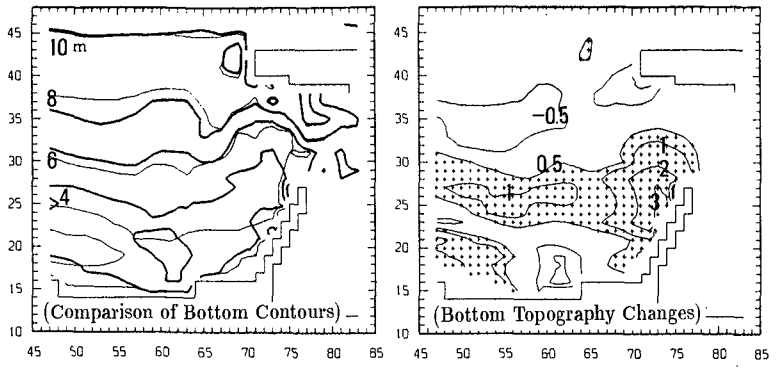

(c) Calculation (Nearshore Current+Undertow+Wave)

Fig. 8 **Comparison of the calculated bottom contours and bottom topography changes during a year with the measured ones.** (Fine Line: Initial Contour; Bold Line: Contour After a Year)

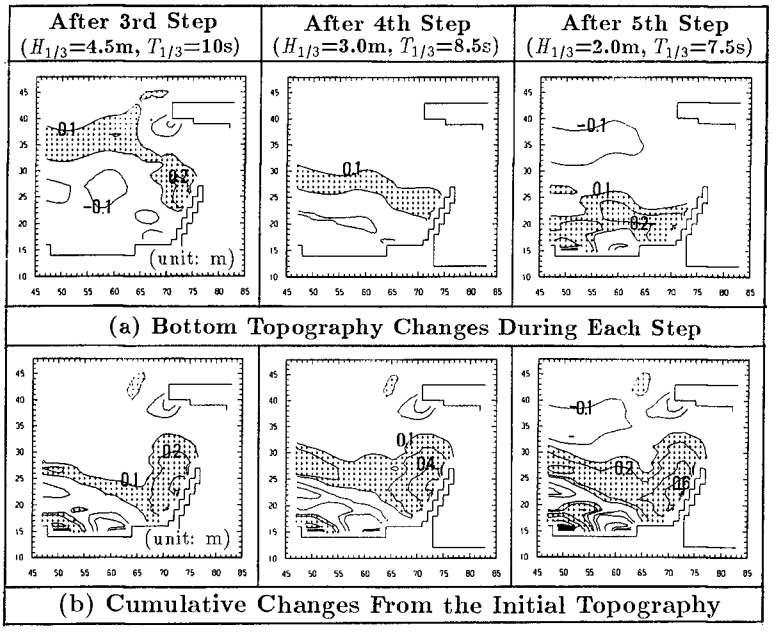

Fig. 9 Examples of calculated bottom topography changes by taking into account the sediment transport due to nearshore currents, undertows and waves.

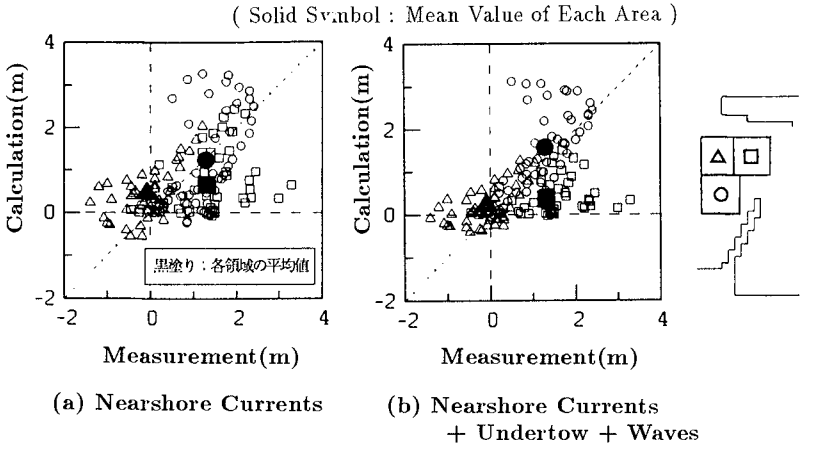

Fig. 10 Comaprisons between the measured and the calculated bottom elevation changes.

important role in the short-term beach profile change.

The above tendencies of the actual beach profile change can be reproduced well by numerical simulation. However, the reason for disagreement of final topography after a year is that the modelled series of waves are not given continuously and the duration of each step is not appropriate. In order to properly estimate the beach profile changes due to cross-shore sediment transports, more detailed modelling of the storm is needed.

Fig. 10 shows the comparisons between the measured and the calculated bottom elevation changes. The solid symbols indicate the mean values in each area and the open symbols indicate those at each calculation point. Although the results at each point scatter a lot, the averaged values of each area around the harbor entrance show reasonable agreements in both cases.

CONCLUSIONS

The results of this study are summarized as follows:

(1) The parabolic equation model has a fairly good accuracy for estimating the random wave transformation such as combined diffraction, refraction and wave breaking.

(2) The undertow was clearly observed through the field investigation. A simple vector addition of the nearshore current vector and the undertow vector has enough accuracy for practical use for estimating the near-bottom mean current in the surf zone.

(3) For a long-term beach evolution, the measurement showed that beach profile changes due to cross-shore sediment transports were cancelled and the beach evolution can be reproduced satisfactorily by taking into account only the sediment transport due to nearshore currents. Further investigations are, however, needed for properly estimating the short-term beach profile changes due to waves and undertow as well as the long-term beach evolution due to nearshore currents.

REFERENCES

Goda, Y., 1970: A synthesis of breaker indices, *Trans. Japan Soc. Civil Engrs.*, Vol.2, Part2, pp.227-230.

Isobe, M., 1987: A parabolic equation model for transformation of irregular waves due to refraction, diffraction and breaking, *Coastal Eng. in Japan*, Vol. 30, No. 1, JSCE, pp.33-47.

Sato, S., M. Fukuhama and K. Horikawa, 1988: Measurements of near-bottom velocities under random waves on a constant slope, *Coastal Eng. in Japan*, Vol. 31, No. 2, JSCE, pp.219-229.

Shimizu, T., H. Nodani and K. Kondo, 1990: Practical application of the three-dimensional beach evolution model, *Proc. 22nd Int. Conf. on Coastal Eng.*, ASCE, pp.2481-2494.

Shimizu, T., A. Ukai and M. Isobe 1992: Field verification of numerical models for calculation of nearshore wave field, *Proc. 23rd Int. Conf. on Coastal Eng.*, ASCE, pp.590-603.

Shimizu, T. , A. Ukai, Y. Kubo and M. Shimada, 1994: Field applicability of wave models to estimating the wave fields outside and inside a harbor, *Proc. HYDRO-PORT'94*, pp.303-315.

Svendsen, I.A. and R.S. Lorenz, 1989: Velocities in combined undertow and longshore currents, *Coastal Eng.*, Vol.13, pp.57-79.

Tanaka, H. and N. Shuto, 1981: Friction coefficient for a wave-current coexistent system, *Coastal Eng. in Japan*, Vol.24, JSCE, pp.105-128.

Watanabe, A., Y. Riho and K. Horikawa, 1980: Beach profile and on-offshore sediment transport, *Proc. 17th Int. Conf. on Coastal Eng.*, pp.1106-1121.

Watanabe, A., 1982: Numerical models of nearshore currents and beach deformation, *Coastal Eng. in Japan*, Vol.25, JSCE, pp.147-161.

Watanabe, A., K. Maruyama, T. Shimizu and T. Sakakiyama, 1986: Numerical prediction model of three-dimensional beach deformation around a structure, *Coastal Eng. in Japan*, Vol.29, JSCE, pp.179-194.

Watanabe, A., T. Shimizu and K. Kondo, 1991: Field application of a numerical model of beach topography change, *Proc. of Coastal Sediments '91*, ASCE, pp.1814-1828.